

## Collisionless Plasma Shocks in Striated Electron Temperatures

P. Guio<sup>1</sup> and H. L. Pécseli<sup>2</sup>

<sup>1</sup>*Department of Physics and Astronomy, University College London, Gower Street, London WC1E 6BT, United Kingdom*

<sup>2</sup>*University of Oslo, Department of Physics, Box 1048 Blindern, N-0316 Oslo, Norway*

(Received 8 January 2010; published 26 February 2010)

The existence of low frequency waveguide modes of ion acoustic waves is demonstrated in magnetized plasmas for electron temperatures striated along the magnetic field lines. At higher frequencies, in a band between the ion cyclotron and the ion plasma frequency, radiative modes develop and propagate obliquely to the field away from the striation. Arguments for the subsequent formation and propagation of electrostatic shock are presented and demonstrated numerically. For such plasma conditions, the dissipation mechanism is the “leakage” of the harmonics generated by the wave steepening.

DOI: [10.1103/PhysRevLett.104.085002](https://doi.org/10.1103/PhysRevLett.104.085002)

PACS numbers: 52.35.Tc, 52.35.Fp, 52.65.-y

The formation of shocks as described by Burgers’ equation [1] can be understood as a balance between the energy input by an external source (a piston moving with velocity  $U$ , for instance) and viscous dissipation, with kinematic viscosity coefficient  $\nu$ . In one spatial dimension, this nonlinear problem can be solved exactly by a Cole-Hopf transformation to demonstrate, for instance, that the shock thickness varies as  $\sim \nu/U$  with the basic parameters of the problem. In principle, Burgers’ equation can apply for any continuous viscous fluid media, also plasmas. Experiments performed in the strongly magnetized plasma of the Risø  $Q$  machine [2] demonstrated that for moderate electron to ion temperature ratios  $T_e/T_i$ , the strong ion Landau damping prohibited the formation of shock. For large temperature ratios, the ion Landau damping is reduced, and there is a possibility for forming steady state nonlinear shocklike forms, propagating at a constant speed [2,3].

In the present study we present a novel mechanism of an effective energy dissipation, selective radiation or “leakage” of short wavelength ion sound waves. We also demonstrate that electrostatic shocks can form as a balance between these losses and the standard nonlinear wave steepening as described by the nonlinear term in the “simple wave” equation,  $\partial u/\partial t + u\partial u/\partial z = 0$ , [1,4]. Studies in two spatial dimensions are sufficient for illustrating the basic ideas, and the analysis of the present Letter is restricted to 2D.

Magnetized plasmas are considered here for conditions where the electron temperature  $T_e$  varies in the direction perpendicular to an externally imposed homogeneous magnetic field [5,6]. Such conditions occur often in nature for plasmas out of equilibrium [7]. For the present analysis it is essential that the ion cyclotron frequency is smaller than the ion plasma frequency, i.e.,  $\Omega_{ci} < \Omega_{pi}$ . The relevant frequencies are assumed to be so low that an inertialess electron component can be taken to be in local Boltzmann equilibrium at all times. We assume quasineutrality,  $n_e \approx n_i$ . For a linearized fluid model, we readily

derive a basic equation in the form

$$\frac{\partial^4}{\partial t^4} \psi - \frac{T_e(x)}{M} \frac{\partial^2}{\partial t^2} \left( \nabla_{\perp}^2 + \frac{\partial^2}{\partial z^2} \right) \psi + \Omega_{ci}^2 \frac{\partial^2}{\partial t^2} \psi - \Omega_{ci}^2 \frac{T_e(x)}{M} \frac{\partial^2}{\partial z^2} \psi = 0, \quad (1)$$

where  $\psi$  is the electrostatic potential, related to the relative density perturbations as  $e\psi/T_e = \eta \equiv n_1/n_0$ . Since we are here only interested in cases where  $T_e/T_i \gg 1$ , we took  $T_i = 0$  in (1). In case  $T_e = \text{const}$ , a linear dispersion relation is readily obtained from (1) by Fourier transforming with respect to time and space. This dispersion relation contains two branches, one for  $\omega < \Omega_{ci}$  and one for  $\Omega_{ci} < \omega < \Omega_{pi}$ , the latter containing also the ion cyclotron waves. The wave properties of the two branches are very different, as illustrated best by the angle between the group velocity and the wave vector [6]. For very low frequencies,  $\omega \ll \Omega_{ci}$ , these two vectors are almost perpendicular, while they are close to parallel when  $\omega \gg \Omega_{ci}$ . In the limit  $k_{\perp} \rightarrow 0$ , the dispersion relation reduces to  $(\omega^2 - \Omega_{ci}^2) \times (\omega^2 - k^2 C_s^2) = 0$  containing ion sound waves and the electrostatic ion cyclotron resonance.

If we let  $T_e = T_e(x)$ , with  $z$  along the magnetic field  $\mathbf{B}$  and  $x$  in the transverse direction, we can still Fourier transform with respect to time and the  $z$  direction. We denote the Fourier transformed electrostatic potential by  $\hat{\psi}$ . Normalizing frequencies and lengths so that  $\Omega \equiv \omega/\Omega_{ci}$  and  $\xi \equiv x\Omega_{ci}/C_s$ , respectively, we readily obtain the expression

$$\frac{d^2}{d\xi^2} \hat{\psi} = (\Omega^2 - 1) \left( \frac{1}{\gamma^2} - \frac{T_0}{T_e(\xi)} \right) \hat{\psi}, \quad (2)$$

where we introduced a normalized propagation speed  $\gamma^2 \equiv (\omega/k_z)^2 (M/T_0)$ , and  $T_0$  is a reference temperature. Thus,  $\gamma$  measures the ratio between the phase velocity along the magnetic field and a sound speed, so that  $\gamma = \text{const}$  would correspond to exactly nondispersive wave propagation. The expression (2) has the form of an eigenvalue equation,

with  $1/\gamma^2$  being the eigenvalue. We present numerical solutions in Fig. 1. In the low frequency limit  $\omega < \Omega_{ci}$ , shown in the middle panel, the waves are confined to the electron temperature striation (here denoted “waveguide modes”), corresponding to a discrete set of eigenfunctions  $\hat{\psi}_m$ , with mode number  $m$ . For the Gaussian profile  $T_e(x)$  considered here, the mode number  $m$  corresponds to the number of zero-crossing of  $\hat{\psi}_m(x)$  [6]. For the three-dimensional problem we would have *two* indexes  $\hat{\psi}_{km}$  corresponding to the two directions perpendicular to  $\mathbf{B}$ . From  $\hat{\psi}_m$  we can obtain the corresponding eigenmodes for the  $\mathbf{B}$ -parallel velocity  $u_{\parallel}$ . The value of  $\gamma$  depends on  $\Omega$ , and we find for  $\Omega = 0, \frac{1}{4}, \frac{1}{2}, \frac{3}{4}$ , that  $\gamma_0^2 = 1.3942, 1.3805, 1.3311$ , and  $1.2006$ , i.e., a relatively weak variation of  $\gamma_0$  with  $\Omega$ . We note also that the eigenfunctions change only little in spite of the large change in  $\Omega$ . Only for  $\Omega$  close to unity, say around 0.9 or larger, do we see significant variations in  $\hat{\psi}_0(x)$  and  $\gamma_0$ . For shallow temperature variations and narrow temperature ducts, we have only the lowest order mode  $\hat{\psi}_0(x)$ . For  $\gamma$  smaller than the minimum value of  $T_e(x)/T_0$  we have a continuum of eigenvalues with corresponding eigenfunctions. In all cases we used  $T_0 \equiv \frac{1}{2}(T_e(0) + T_e(|\infty|))$ .

For  $\omega > \Omega_{ci}$  the right-hand side of (2) changes sign, and the nature of the eigenmodes changes as well, to become free modes as seen in the lower panel in Fig. 1. If we let the electron temperature striation vanish to have a uniform  $T_e$ , then the free modes degenerate to two obliquely propagating plane waves.

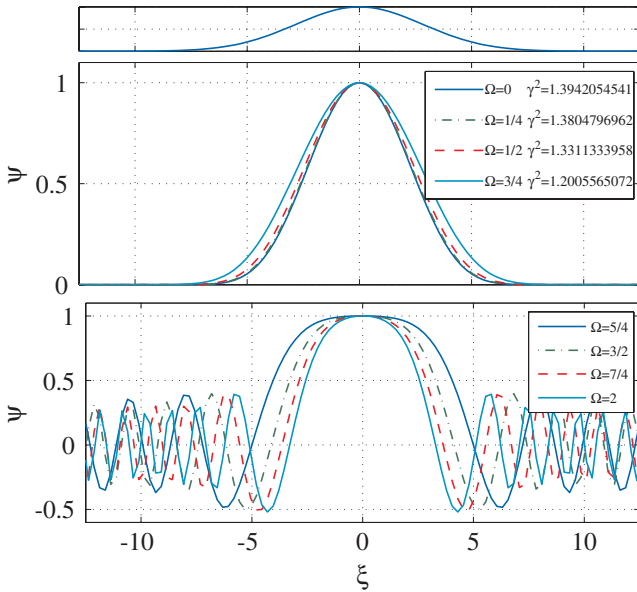


FIG. 1 (color). Illustrative examples of numerical solutions of (2) for the electron temperature profile shown in the upper panel, and defined by  $T_e(\xi)/T_0 = 1 - \frac{1}{2}\mathcal{D} + \mathcal{D}\exp(-\xi^2/\mathcal{W}^2)$ , where  $\mathcal{W} = 4$  and  $\mathcal{D} = 24/23$ . Waveguide mode solutions for  $\Omega = 0, \frac{1}{4}, \frac{1}{2}, \frac{3}{4}$  are shown in the middle panel. Free modes solutions obtained for  $\Omega = \frac{5}{4}, \frac{3}{2}, \frac{7}{4}, 2$  and  $\gamma = 2$  are shown in the lower panel.

We consider now the low frequency limit of the branch of dispersion relation with  $\omega < \Omega_{ci}$ . For  $m > 1$ , the waveguide modes can decay for one  $m$  value to modes with other  $m$  values. The  $m = 0$  mode has no decay to other forward propagating modes, and will be the one considered here. For this highest phase velocity mode, with eigenmode  $\hat{\psi}_0(x)$ , wave steepening will be the dominant nonlinearity [1,4]. The nonlinear terms couple the various modes to give products of  $x$  modes. These can be expanded as, for instance,  $\hat{\psi}_i(x)\hat{\psi}_j(x) = \sum_q \zeta_{qij} \hat{\psi}_q(x)$ , where we assume that by including the continuum part the set  $\hat{\psi}_m$  is complete and orthonormal [8]. For the lowest order waveguide mode we have, in particular,  $\zeta_{j00} = \int_{-\infty}^{\infty} \hat{\psi}_0^2(x)\hat{\psi}_j(x)dx$ . For a large class of relevant electron temperature profiles we can ignore all higher order modes, and retain only  $\hat{\psi}_0$ , and introduce here  $\zeta_0 \equiv \int_{-\infty}^{\infty} \hat{\psi}_0^3(x)dx$ . For the Gaussian variations of  $T_e(x)$  studied here, we will have  $\zeta_0 > \zeta_j$  for all  $j \geq 1$ , since  $\hat{\psi}_0$  is the only eigenfunction that is positive everywhere. To lowest order in the present low frequency limit we have the relation  $e\hat{\psi}/T_e = \hat{\eta} \approx \hat{u}_{\parallel}/C_s$  between fluctuations in relative density and the velocity in the  $\mathbf{B}$ -parallel direction. Our arguments concerning the mode structure therefore apply to the velocity variations as well.

Considering the limit of time scales much larger than the ion cyclotron period, we find after some algebra the result

$$\frac{\partial u_{\parallel}}{\partial t} + (\zeta_0 u_{\parallel} \pm \zeta_T C_{s0}) \frac{\partial u_{\parallel}}{\partial z} = 0, \quad (3)$$

with  $u_{\parallel} = u_{\parallel}(z, t)$ , where the numerical value of  $\zeta_T$  is that of  $\gamma_0$  in the limit of  $\Omega \rightarrow 0$ . Small polarization drifts  $\perp \mathbf{B}$  are ignored. We introduced a constant reference sound speed  $C_{s0}$ . We anticipate that  $\zeta_T$  is here not much different from  $\zeta_0$ , since the form of  $\hat{\psi}_0(x)$  is close to  $T_e(x) - T_e(|\infty|)$ . The solutions of (3) have the well-known steepening of the initial condition. The characteristic time for wave breaking is approximately  $\mathcal{L}/\max\{u_{\parallel}(t=0)\}$ , where  $\mathcal{L}$  is the characteristic scale length of the initial perturbation along  $\mathbf{B}$  and  $\max\{u_{\parallel}(t=0)\}$  is the maximum value of the initial velocity perturbation. The model Eq. (3) assumes  $\hat{\psi}_0(x)$  and  $\gamma_0$  being used also when  $\Omega > 0$ , but this approximation is acceptable for at least  $0 \leq \Omega < 0.75$ , as seen in the middle panel in Fig. 1. For the basic ideas outlined in the present work, this restriction is of little consequence. Polarization drifts become increasingly larger as  $\Omega$  is increased, but these do not affect the dynamics parallel to  $\mathbf{B}$ , which is covered by (3).

If we initialize the system with characteristic wavelengths corresponding to frequencies  $\omega \ll \Omega_{ci}$ , i.e.,  $\mathcal{L} \gg C_s/\Omega_{ci}$ , the short time evolution will be governed by (3), and we will have shorter and shorter scales developing as for the usual breaking of waves [1,4]. This process is, however, arrested when the characteristic length scales become of the order of the effective ion Larmor radius  $C_s/\Omega_{ci}$ , where the modes become radiating, and are no longer confined to the waveguide. We propose a phenome-

nological expression for the process, best written in Fourier space in a frame moving with  $C_{s0}$ , as

$$\frac{\partial \hat{u}_{\parallel}}{\partial t} + i \frac{\zeta_0 k_{\parallel}}{2} \hat{u}_{\parallel} \otimes \hat{u}_{\parallel} = - \frac{\hat{u}_{\parallel}}{\mathcal{T}(k_{\parallel})} \mathcal{H}\left(|k_{\parallel}| - \frac{\Omega_{ci}}{C_{s0}}\right), \quad (4)$$

with  $\hat{u}_{\parallel} = \hat{u}_{\parallel}(k_{\parallel}, t)$ . The symbol  $\otimes$  denotes the convolution product and  $\mathcal{H}$  is Heaviside's step function.  $\mathcal{T}$  characterizes the time it takes for the energy of the  $\omega > \Omega_{ci}$  waves to be lost from the waveguide. We have  $\mathcal{T} = \mathcal{T}(k_{\parallel})$ , but it will depend also on parameters such as the waveguide width as well as the other plasma parameters. We expect that increasing width gives increasing  $\mathcal{T}$ , i.e., decreasing shock thickness  $\Delta$ . Within the present model the waveform will steepen uninhibited until the shock thickness becomes of the order of  $C_s/\Omega_{ci}$ , at which time the harmonic frequencies will exceed  $\Omega_{ci}$  to become radiative and the high frequency wave energy is lost from the waveguide. Consequently, the  $\mathbf{B}$ -parallel scale of the shock is controlled by a quantity referring to the  $\mathbf{B}$ -perpendicular dynamics.

We study the nonlinear propagation of low frequency waves in an electron temperature striated magnetized plasma numerically by using a  $2\frac{1}{2}$ -dimensional particle in cell (PIC) code described elsewhere [6]. The code assumes explicitly the electrons to be locally Boltzmann distributed and the resulting nonlinear Poisson equation is solved by iteration. We use a Gaussian variation for  $T_e(x)$  so that  $T_e(|\infty|)/T_i = 1$ , while  $T_e(0)/T_i > 1$ , where  $T_i = \text{const}$ . The width of the electron striation is here  $\mathcal{W} = 28\lambda_{Di} = 3.9C_{s0}/\Omega_{ci}$ . Several values of  $T_e(0)/T_i$  were investigated.

Results illustrating the waveguide and the free modes are shown in Fig. 2. The properties are clearly different and consistent with the interpretation given before. The waveguide modes are confined to the electron striation, while the high frequency free modes are dispersing or “leaking”, consistent also with laboratory experimental results [5]. It is important to emphasize that this apparent damping will be found also in a fluid model. The observed effective damping is caused by wave energy dispersing in space, and dissipated by linear ion Landau damping outside the electron temperature striations where  $T_e(|\infty|)/T_i = 1$  in all cases considered. Each step in the process is formally time reversible. In order to emphasize the physical effects we discuss here, we consider only high temperature ratios,  $T_e(0)/T_i \geq 25$ , in order to reduce the effects of linear as well as nonlinear ion Landau damping. Such high temperature ratios (even as large as  $T_e/T_i = 100$ ) can be obtained in discharge plasmas under laboratory conditions [9]. For nonlinear waves described by a Korteweg–de Vries (KdV) equation, a shocklike structure is followed by Airy-type ripples, originating from the dispersion term in the KdV equation. These ripples are absent in our results, see Fig. 3. Likewise, at the high temperature ratio used here (with  $C_{s0} \gg u_{th,i}$ , the ion thermal velocity), we find no ions

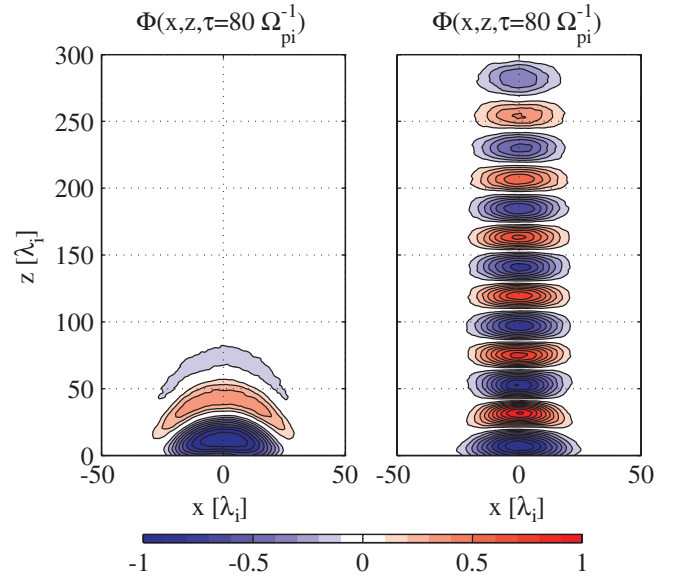


FIG. 2 (color). Examples of numerical simulations showing the variations of the normalized potential  $\Phi = e\psi/T_i$  as a function of position at a fixed time. The electron temperature enhancement is localized as a Gaussian in the  $x$  direction. We have  $\omega = \Omega_{pi}\pi/5$  in both cases while  $\Omega_{ci}/\Omega_{pi} = 0.05$  and  $\Omega_{ci}/\Omega_{pi} = 1$  in the left and right panels, respectively. We have here  $T_e/T_i = 50$ . For clarity, only a part of the simulation domain is shown.

being reflected by the shock. A backward propagating rarefaction wave is of no concern here.

In Fig. 3 we show an example of the formation and propagation of a shock. The initial density has an error

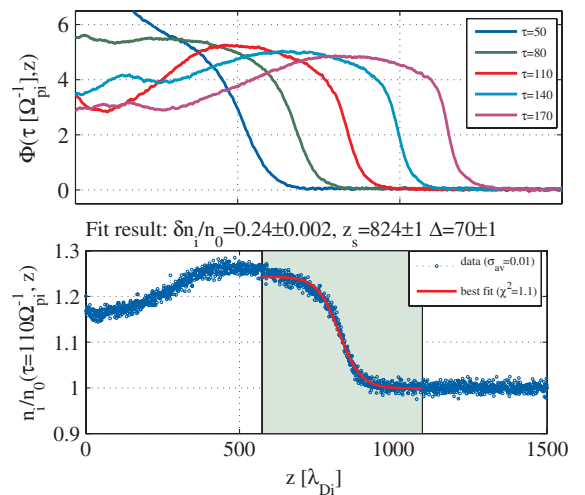


FIG. 3 (color). Numerical simulation showing normalized potential  $\Phi = e\psi/T_i$  and relative density  $n_i/n_0$  during the formation and propagation of a shock under the conditions mentioned before. We have  $T_e/T_i = 25$ ,  $\Omega_{ci}/\Omega_{pi} = \frac{1}{2}$  and  $\delta n_i/n_0 \approx 0.24$ , where  $\delta n_i$  is the actual detected density perturbation at the time where the shock is fully formed. The background density  $n_0$  is normalized to unity. Lower frame shows example of shock fitting for the ion density.

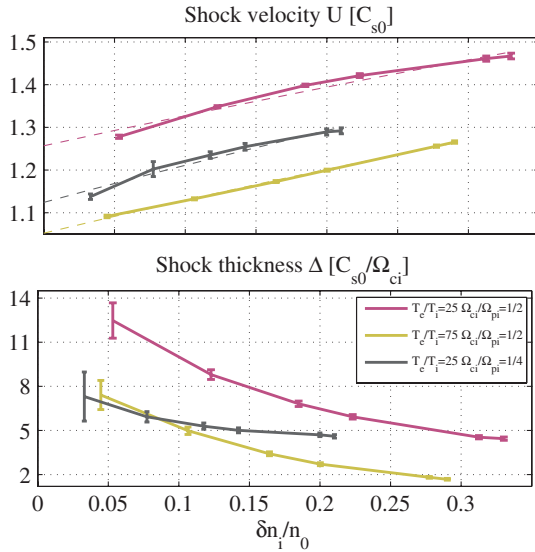


FIG. 4 (color). Shock velocity  $U$  in units of  $C_{s0}$  (upper panel) and saturated shock thickness  $\Delta$  in units of  $C_{s0}/\Omega_{ci}$  (lower panel) as function of the fully formed shock relative height  $\delta n_i/n_0$ , for different combinations of the parameters  $T_e/T_i = 25$  and  $75$ , and  $\Omega_{ci}/\Omega_{pi} = \frac{1}{4}$  and  $\frac{1}{2}$ .

function type spatial variation in the  $\mathbf{B}$ -field aligned direction. Ions are continuously injected at the boundary at  $z = 0$  to maintain the energy input. We have  $T_e/T_i = 25$ ,  $\Omega_{ci}/\Omega_{pi} = \frac{1}{2}$  and  $\delta n_i/n_0 \approx 0.24$ , where  $\delta n_i$  refers to the actual detected density perturbation at the time where the shock is fully formed, and not to the initial imposed perturbation. The standard deviation of the parameters is estimated from fitting the shock profile with a nonlinear Levenberg-Marquardt method.

In Fig. 4 we show the shock thickness  $\Delta$  and the normalized shock velocity  $U$  for various combinations of the parameters  $T_e/T_i$ ,  $\Omega_{ci}/\Omega_{pi}$  and  $\delta n_i/n_0$ . The velocity  $U$  is obtained by following the shock position  $z_s$  as function of time. For small or moderate values of  $\delta n_i/n_0$  we find a close to linear relationship between  $\delta n_i$  and  $U$ . As  $\delta n_i \rightarrow 0$  (shown with a dashed line fit) we have  $U$  approaching the appropriate value for  $\gamma_0$ , apart from small corrections due to finite  $T_i$  ignored in (2). For  $\Omega_{ci}/\Omega_{pi} = \frac{1}{2}$  we find that an approximate fivefold increase in  $\delta n_i/n_0$  corresponds to approximately 50% reduction in  $\Delta$ . We demonstrated

also that the shock thickness  $\Delta$  scales inversely proportional to the width of the striation. We verified that changes in the initial  $\mathbf{B}$ -parallel scale length of the initial density profile do not change the saturated shock thickness  $\Delta$  for any  $\delta n_i/n_0$ . We studied also a weak magnetic field limit, with  $\Omega_{ci}/\Omega_{pi} = \frac{1}{4}$ . Here, finite ion Larmor radius effects [ignored in deriving (1)] begin to be important, since the striation is now only  $\sim 10$  ion Larmor radii wide. For this limit we find that  $\Delta$  is almost constant. Even weaker magnetic fields will require a fully kinetic theoretical analysis to account for the effects of collisionless ion gyroviscosity [10].

We here reported arguments for the formation of shocks in electron striations in magnetized plasmas when  $\Omega_{ci} < \Omega_{pi}$  and  $T_e \gg T_i$ . By PIC simulations we demonstrated the formation and propagation of electrostatic shocks under these conditions for a wide combination of parameters. The decreasing shock thickness for increasing amplitudes is found also for classical shocks as described by Burgers' equation, but in our case the dissipation mechanism is leakage from the electron temperature striation of the short scale lengths generated by the nonlinear wave steepening. The ideas presented here can have wider applications.

- 
- [1] G. B. Whitham, *Linear and Nonlinear Waves* (John Wiley & Sons, New York, 1974).
  - [2] H. K. Andersen, N. D'Angelo, P. Michelsen, and P. Nielsen, Phys. Rev. Lett. **19**, 149 (1967).
  - [3] H. Ikezi, T. Kamimura, M. Kako, and K. E. Lonngren, Phys. Fluids **16**, 2167 (1973).
  - [4] D. T. Blackstock, in *American Institute of Physics Handbook* (McGraw-Hill, New York, 1972), 3rd ed. pp. 3–183.
  - [5] Y. Nishida and A. Hirose, Phys. Plasmas **19**, 447 (1977).
  - [6] P. Guio, S. Børve, H. L. Pécseli, and J. Trulsen, Ann. Geophys. **18**, 1613 (2001).
  - [7] J. R. Peñano, G. J. Morales, and J. E. Maggs, Phys. Plasmas **7**, 144 (2000).
  - [8] W. M. Manheimer, Phys. Fluids **12**, 2426 (1969).
  - [9] K. Takahashi, T. Oishi, K. Shimomai, Y. Hayashi, and S. Nishino, Phys. Rev. E **58**, 7805 (1998).
  - [10] S. I. Braginskii, in *Reviews of Plasma Physics*, edited by M. A. Leontovich (Consultants Bureau, New York, 1965) Vol. 1, pp. 205–311.